

On the implementation of gain-scheduled LPV control for oxygen stoichiometry regulation in PEM fuel cells

F.D. Bianchi, C. Kunusch, *Member, IEEE*, C. Ocampo-Martinez, *Member, IEEE*,
and R.S. Sánchez-Peña, *Senior Member, IEEE*

Abstract—The article addresses the LPV control of a Polymer Electrolyte Membrane Fuel Cell (PEMFC) facing oxygen stoichiometry regulation. In order to optimize efficiency, PEMFCs require reliable control systems ensuring stability and performance, as well as robustness to model uncertainties and external perturbations. On the other hand, PEMFC systems present highly nonlinear behaviors that demand nonlinear and/or adaptive control strategies to achieve high performance in the entire operating range. Here, a linear parameter varying (LPV) gain scheduled control is proposed. The control is based on a piecewise affine LPV representation of the PEMFC, a model that can be available in practice. The control strategy is applied to a couple of experimental practical situations in a laboratory fuel cell system, to evaluate not only the performance but also the difficulties that can arise in real applications.

I. INTRODUCTION

The current increasing of pollution reduction demands is driving innovation on clean energy sources. Among these, fuel cells (FCs) are regarded as one of the most promising technologies, due to their potential efficiency, compactness and reliability [1]. Particularly, Polymer Electrolyte Membrane Fuel Cells (PEMFCs) are electrochemical devices that generate electrical energy from hydrogen and oxygen, with pure water and heat as by-products. Considering that hydrogen is widely available and can be obtained from many renewable sources using solar and wind energy, FCs represent an attractive, feasible alternative to reduce fossil fuel dependence. However, the widespread use of hydrogen as fuel –and the resulting *hydrogen economy*– despite its interesting possibilities, has some technological issues to be solved. In spite of recent advances, their relatively high costs, suboptimal efficiency and reduced lifetime remain as major limitations. For this reason, together with the continuous improvement of materials and components, the incorporation of advanced control strategies embodies a major technological issue, in order to achieve cost reduction, performance improvement and efficiency optimization. In the light of these considerations, it becomes clear that in order to optimize efficiency, reliable control systems ensuring stability and performance, as well as robustness against model uncertainties and external perturbations are

of capital importance for PEMFC success. In particular, the oxygen stoichiometry control system [2], [3], [4], has to be able to optimize the system conversion efficiency, avoiding performance deterioration together with eventual irreversible damages in the polymeric membranes, due to oxygen starvation. As a novel solution to this technological problem, a robust oxygen stoichiometry control design and its implementation in a laboratory FC system are presented in this work. In particular, a linear parameter varying (LPV) gain scheduled control strategy based on a set of local models is designed and tested experimentally.

For the application presented on this paper, the LPV approach has several advantages compared to other techniques, e.g., (i) it derives from the robust control framework, therefore model uncertainty and bounded perturbations sets are naturally included and stability/performance guarantees are provided; (ii) LPV method has proven robust stability and performance guarantees based on linear matrix inequalities (LMI) convex optimization, useful issues facing the nonlinear nature of the plant dynamics; and (iii) the time-varying controller update is based solely on the variable measurements, which is critical due to the fast dynamics of this application. This latter fact provides a prompt response, as opposed to adaptive control or model predictive control (MPC), which are based on real-time identification or optimization, respectively, more suitable for slower dynamics, e.g., process control. However, some approaches that consider explicit MPC controllers [5] or MPC emulators [6] are reported for real-time control of PEMFCs. These approaches avoid online optimization, but are based on linear time-invariant models, and that significantly increases the complexity of the controller.

Only few preliminary approaches have been reported in the literature regarding LPV on FCs. In fact, the use of LPV techniques for FCs is considered for performing control-oriented models [7], [8], designing LPV-based controllers [9], and developing fault diagnosis methodologies based on LPV observers [10]. Related to FC modeling, in [7] the usefulness of the LPV model structure is explored for model reduction of a detailed physical model of a solid-oxide FC stack. The results of this work reported the suitable adjustment of the reduced LPV models to the behavior shown by a high-order physics-based model of the system. On the other hand, an LPV control approach for FCs is reported in [9]. There, affine quasi-LPV models were firstly defined for identified models of the stack voltage and the air compressor flow of a PEMFC. Then, the design of an LPV controller for dis-

F.D. Bianchi is with Catalonia Institute for Energy Research, IREC, Jardins de les Dones de Negre 1, 08930 Sant Adrià de Besòs, Barcelona, Spain. e-mail: fbianchi@irec.cat

C. Kunusch and C. Ocampo-Martinez are with Institut de Robòtica i Informàtica Industrial (CSIC-UPC), Llorens i Artigas, 4-6, 08028 Barcelona, Spain.

R.S. Sánchez-Peña is with CONICET and Instituto Tecnológico de Buenos Aires (ITBA), Av. Madero 399, (C1106ACD) Buenos Aires, Argentina.

turbance rejection and the tracking control problem and the discussion of simulation results are presented. Notice that, in the best of the author's knowledge, these few references represent the current literature concerning the application of LPV techniques to FC based systems. None of them present experimental results of controller implementation, which in fact represent a very relevant contribution of this paper.

The proposed LPV control is based on local linear models of the nonlinear dynamics and produces a set of linear controllers interpolated in order to obtain the global control algorithm. This approach is especially useful for complex systems where analytic LPV models are difficult or impossible to obtain.

The paper is organized as follows. Section II describes the physical system and Section III the LPV framework and the controller as well as their discretization. Section IV presents the experimental results in two different practical scenarios, and Section V closes the work with final conclusions.

Notation: \mathbb{R} (\mathbb{C}) is the set of real (complex) numbers and $\mathbb{R}^{n \times m}$ the set of real matrices of $n \times m$. The Kronecker product is represented by \otimes . For a symmetric matrix $X \in \mathbb{R}^{n \times n}$, $X > 0$ ($X < 0$) denotes positive (negative) definiteness. Given symmetric matrices X , Y and a general matrix Z , the following notation will be used, $Z + Z^T = Z + (\star)$ and

$$\begin{bmatrix} X & Z \\ Z^T & Y \end{bmatrix} = \begin{bmatrix} X & \star \\ Z^T & Y \end{bmatrix}.$$

II. SYSTEM PHYSICAL DESCRIPTION

Concisely, the laboratory test plant under consideration mainly comprises a central PEMFC stack and ancillary units. Details of the laboratory test station are shown in a schematic diagram of the system depicted in Figure 1, where the main subsystems are briefly described as follows:

- Air Compressor: 12 V DC oil-free diaphragm vacuum pump. The input voltage of this device is used as the control action.
- Hydrogen and Oxygen humidifiers and line heaters: these are used to maintain proper humidity and temperature conditions inside the cell stack, an important issue for PEM membranes. Cellkraft® membrane exchange humidifiers are used in the current set-up. Decentralized PID controllers ensure adequate operation values.
- FC stack: an ZBT® 8-cell stack with Nafion 115® membrane electrode assemblies (MEAs) is used, 50 cm² of active area and 150 W power.

In the sequel, the following modeling assumptions have been considered [11], [12]:

- A mass flow control device (W_{H_2}) ensures a constant hydrogen stoichiometry supply.
- An auxiliary control system efficiently regulates gas temperatures at five points of the plant: cathode and anode humidifiers ($T_{hum,ca}$ and $T_{hum,an}$), cathode and anode line heaters ($T_{lh,ca}$ and $T_{lh,an}$) and stack (T_{st}).
- A humidity control loop regulates the water injection of the humidifiers to a relative level close to 100 %.

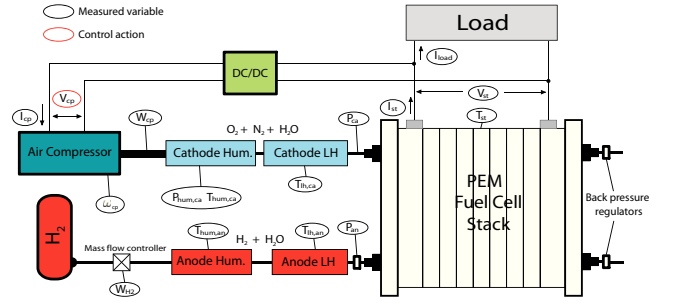


Fig. 1. Schematic diagram of the PEMFC based generation system (FCGS)

- The FC model is one dimensional, so the gases and reactions are considered uniformly distributed in the cell.
- The electrochemical properties are evaluated at the average stack temperature (70°C), so temperature variations across the stack are neglected.
- The water entering the cathode and anode is only in the vapor phase.
- The effects of liquid water creation are negligible at the gas flow model level.
- The water activity is uniform across the membrane and is in equilibrium with the water activity at the cathode and anode catalyst layers.

The nonlinear model of the plant under study was already developed and validated in [11]. In general terms, the modeling process was conducted following a modular methodology, combining a theoretical approach, together with empirical analysis based on experimental data. Taking the state vector $\tilde{x} \in \mathbb{R}^7$ of the complete nonlinear model, the control input for the current study is the compressor voltage $v = V_{cp} \in \mathbb{R}$, the external disturbance is the stack current $I_{st} \in \mathbb{R}$ and the output is the inlet stoichiometry $\lambda_{O_2} \in \mathbb{R}$. Accordingly, the system can be represented by the following continuous-time state-space model:

$$\dot{\tilde{x}}(t) = f(\tilde{x}(t), t) + g(\tilde{x})v(t), \quad (1)$$

where $f : \mathbb{R}^8 \rightarrow \mathbb{R}^7$, $g : \mathbb{R}^7 \rightarrow \mathbb{R}^7$, and the state variables are defined as

- $\tilde{x}_1 = \omega_{cp}$: motor shaft angular velocity;
- $\tilde{x}_2 = m_{hum,ca}$: air mass inside the cathode humidifier;
- $\tilde{x}_3 = m_{O_2,ca}$: oxygen mass in the cathode channels;
- $\tilde{x}_4 = m_{N_2,ca}$: nitrogen mass in the cathode channels;
- $\tilde{x}_5 = m_{v,ca}$: vapor mass in the cathode channels;
- $\tilde{x}_6 = m_{H_2,an}$: hydrogen mass in the anode channels;
- $\tilde{x}_7 = m_{v,an}$: vapor mass in the anode channels.

It can be shown that the efficiency optimization of the current system can be achieved by regulating the oxygen mass inflow towards the stack cathode. If an adequate oxidant flow is ensured through the stack, the load demand is satisfied with minimum fuel consumption. Additionally, oxygen starvation and irreversible membrane damage are averted.

To accomplish such an optimal oxidant flow is equivalent to maintaining the oxygen excess ratio of the cathode at an

optimal value. The oxygen excess ratio or oxygen stoichiometry is defined as

$$\lambda_{O_2}(t) = \frac{W_{O_2,ca}(t)}{W_{O_2,react}(t)}, \quad (2)$$

where $W_{O_2,react}(t)$ is the oxygen flow consumed in the reaction and $W_{O_2,ca}(t)$ is the oxygen partial flow entering the cathode, which depends on the air flow released by the compressor $W_{cp}(t)$, i.e.,

$$W_{O_2,ca}(t) = \frac{\chi_{O_2} W_{cp}(t)}{1 + \omega_{amb}(t)}, \quad (3)$$

being $\omega_{amb}(t)$ the ambient air humidity ratio and χ_{O_2} the molar fraction of oxygen in the air ($\chi_{O_2} = 0.21$).

Notice that $W_{O_2,react}(t)$ is directly related to the stack current in the form

$$W_{O_2,react}(t) = G_{O_2} \frac{n I_{st}(t)}{4F}, \quad (4)$$

with G_{O_2} the molar mass of oxygen, n the number of cells and Faraday's constant F .

As presented in the validated model [11], the two actual system inputs are V_{cp} and I_{st} . The former is the control action, while the latter is a measurable disturbance determined by the load. In this context, these two variables represent a natural selection to parameterize the nonlinear system in terms of an LPV system. Therefore, in the following it will be assumed that the parameter space belongs to \mathbb{R}^2 .

The control objectives considered in this article are outlined as follows.

- Tracking of the oxygen stoichiometry $\lambda_{O_2}(t)$ such that

$$\lim_{t \rightarrow \infty} (\lambda_{O_2}(t) - \lambda_{O_2,ref}) = 0, \quad (5)$$

where $\lambda_{O_2,ref}$ corresponds with a given reference for $\lambda_{O_2}(t)$.

- Disturbance rejection, for changes in the measured stack current $I_{st}(t)$.

III. LPV CONTROL OF PEMFCs

The LPV formulation provides synthesis tools that guarantee stability and performance of the closed loop system in all operating conditions considered in the design. However, to obtain these guarantees, analytic expressions to describe the behavior of the nonlinear system are necessary. This is not always possible, especially in cases of complex models based on look-up-table parameters or with very complex mathematical expressions. In many of these cases, such as the PEMFC based system (1), only a set of linear models describing the local behavior at a set of operating points are available. With no additional information, a linear interpolation of the matrices of the model corresponding to the closest points is commonly used to describe the system behavior at intermediate points. In practice, a dense enough grid of points is a good approximation. This kind of LPV systems, known as piecewise affine LPV systems, will be described in the next subsection along with the synthesis procedure. Finally some comments concerning the discretization of the controller are provided.

A. LPV description and control design

Let $\theta \in \mathbb{R}^2$ be a parameter taking values in a polytope $\Theta = [\underline{\theta}_1, \bar{\theta}_1] \times [\underline{\theta}_2, \bar{\theta}_2]$. Assume that the parameter set is partitioned into $(m_1 - 1) \times (m_2 - 1)$ closed rectangles Θ_{ij} 's. Then, the parameter θ can be expressed as

$$\theta(t) = \sum_{i=1}^{m_1} \sum_{j=1}^{m_2} \alpha_{ij}(t) \hat{\theta}_{ij}, \quad (6)$$

where $\hat{\theta}_{ij}$ are the points on a grid

$$\mathcal{G} = \{\hat{\theta}_{ij}, i = 1, \dots, m_1, j = 1, \dots, m_2\}, \quad (7)$$

defining the partition of the rectangles Θ_{ij} 's,

$$\sum_{i=1}^{m_1} \sum_{j=1}^{m_2} \alpha_{ij} = 1 \quad (8)$$

with

$$\alpha_{ij} = \psi \left(\frac{\hat{\theta}_{(i+1)(j+1),1} - \theta_1}{\hat{\theta}_{(i+1)(j+1),1} - \hat{\theta}_{ij,1}} \cdot \frac{\hat{\theta}_{(i+1)(j+1),2} - \theta_2}{\hat{\theta}_{(i+1)(j+1),2} - \hat{\theta}_{ij,2}} \right) \quad (9)$$

and

$$\psi(\vartheta) = \begin{cases} \vartheta, & \text{if } 0 < \vartheta \leq 1, \\ 0, & \text{otherwise.} \end{cases}$$

That is, if $\theta \in \Theta_{ij}$, then θ is expressed as a convex combination of the vertices of the rectangle Θ_{ij} ,

$$\begin{aligned} \theta = & \alpha_{ij} \theta_{ij} + \alpha_{i(j+1)} \theta_{i(j+1)} + \\ & \alpha_{(i+1)j} \theta_{(i+1)j} + \alpha_{(i+1)(j+1)} \theta_{(i+1)(j+1)}. \end{aligned}$$

Then, the system's description is assumed as

$$\begin{bmatrix} \dot{x}(t) \\ z(t) \\ e(t) \end{bmatrix} = \sum_{i=1}^{m_1} \sum_{j=1}^{m_2} \alpha_{ij}(t) \begin{bmatrix} A_{ij} & B_{1,ij} & B_2 \\ C_{1,ji} & D_{11,ij} & D_{12} \\ C_2 & D_{21} & 0 \end{bmatrix} \begin{bmatrix} x(t) \\ w(t) \\ u(t) \end{bmatrix} \quad (10)$$

being $x \in \mathbb{R}^{n_s}$ the states, $z \in \mathbb{R}^{n_z}$ a performance output, $y \in \mathbb{R}^{n_y}$ the measured variable, $w \in \mathbb{R}^{n_w}$ the disturbance and $u \in \mathbb{R}^{n_u}$ the control input. Expression (10) describes the system as an affine LPV model in each rectangle Θ_{ij} and the matrices are piecewise continuous functions of the parameter θ .

With the previous assumption, the gain-scheduled controller

$$\begin{bmatrix} \dot{x}_c(t) \\ u(t) \end{bmatrix} = \sum_{i=1}^{m_1} \sum_{j=1}^{m_2} \alpha_{ij}(t) \begin{bmatrix} A_{c,ij} & B_{c,ij} \\ C_{c,ji} & D_{c,ij} \end{bmatrix} \begin{bmatrix} x_c(t) \\ e(t) \end{bmatrix} \quad (11)$$

should guarantee that the induced \mathcal{L}_2 norm of the operator $T_{zw} : w \rightarrow z$, mapping the disturbance w to the output z , satisfies

$$\|T_{zw}\|_{\mathcal{L}_2} = \sup_{w \neq 0, \theta \in \Theta} \frac{\|z\|_2}{\|w\|_2} < \gamma$$

and the local closed-loop systems have all poles in the LMI region described by the matrices Γ and Υ presented below (see [13] for more details). This is true if there exist two

symmetric positive definite matrices X and Y and matrices $\hat{A}_{c,ij}$, $\hat{B}_{c,ij}$, $\hat{C}_{c,ij}$ and $D_{c,ij}$ such that

$$\begin{bmatrix} X & I \\ I & Y \end{bmatrix} > 0,$$

$$\begin{bmatrix} XA_{ij} + \hat{B}_{c,ij}C_2 + (\star) & \star \\ \hat{A}_{c,ij}^T + A_{ij} + B_2D_{c,ij}C_2 & A_{c,ij}Y + B_2\hat{C}_{c,ij} + (\star) \\ (XB_{1,ij} + \hat{B}_{c,ij}D_{12})^T & (B_{1,ij} + B_2D_{c,ij}D_{21})^T \\ C_{1,ij} + D_{12}D_{c,ij}C_2 & C_1Y + D_{12}\hat{C}_{c,ij} \end{bmatrix} < 0,$$

$$\begin{bmatrix} \star & \star \\ \star & \star \\ -\gamma I_{n_w} & \star \\ D_{11,ij} + D_{12}\hat{D}_{c,ij}D_{21} & -\gamma I_{n_z} \end{bmatrix} < 0,$$

$$\Upsilon^T \otimes \begin{bmatrix} XA_{ij} + \hat{B}_{c,ij}C_2 & \hat{A}_{c,ij} \\ A_{ij} + B_2D_{c,ij}C_2 & A_{c,ij}Y + B_2\hat{C}_{c,ij} \end{bmatrix} + (\star) +$$

$$+ \Gamma \otimes \begin{bmatrix} X & I \\ I & Y \end{bmatrix} < 0$$

for all $i = 1, \dots, m_1$ and $j = 1, \dots, m_2$. The controller matrices are given by

$$\begin{aligned} A_{c,ij} &= N^{-1}(\hat{A}_{c,ij} - X(A_{ij} - B_2D_{c,ij}C_2)Y \\ &\quad - \hat{B}_{c,ij}C_2Y - XB_2\hat{C}_{c,ij})M^{-T}, \\ B_{c,ij} &= N^{-1}(\hat{B}_{c,ij} - XB_2D_{c,ij}), \\ C_{c,ij} &= (\hat{C}_{c,ij} - D_{c,ij}C_2Y)M^{-T}, \end{aligned}$$

where $I - XY = NM^T$ [14].

Piecewise affine LPV systems were introduced by Lim and How [15] in the context of switched LPV systems with the aim of reducing the conservatism of the previous results. This formulation permits to use piecewise discontinuous Lyapunov functions. Here, static Lyapunov functions are used to simplify the implementation of the controller in an industrial computer. Alternatively, Wu, et al. [16] and Apkarian and Adams [14] proposed the use of continuous parameter dependent Lyapunov functions. The performance obtained with this solution strongly depends on the particular selection of the parameter functions. Furthermore, there is no natural selection of these functions when the system is described by a set of LTI models.

In the case of the PEMFC, the LPV description (10) is obtained from the nonlinear model in (1) by linearizing around a set of operating points defined by the mean values of the compressor voltage and stack current, $V_{cp,0}$ and $I_{st,0}$ respectively. Thus, the linear models are parameterized by $\theta = [V_{cp,0} \ I_{st,0}]^T$. Therefore, the Taylor expansion of (1) around each $\hat{\theta}_{ij} \in \mathcal{G}$ is defined as follows

$$G_{ij} : \begin{cases} \dot{x}(t) = A_{ij}x(t) + B_{ij}u(t), \\ y(t) = Cx(t), \end{cases} \quad (12)$$

where $x(t) = \tilde{x}(t) - x_0(\hat{\theta}_{ij})$, $u(t) = v(t) - v_0(\hat{\theta}_{ij})$ and

$$\begin{aligned} A_{ij} &= \left[\frac{\partial f(x(t), t)}{\partial x(t)} \right]_{\hat{\theta}_{ij}}, & B_{ij} &= \left[\frac{\partial g(x(t))}{\partial x(t)} \right]_{\hat{\theta}_{ij}} \\ C &= [1 \ 0 \ 0 \ 0 \ 0 \ 0 \ 0]. \end{aligned}$$

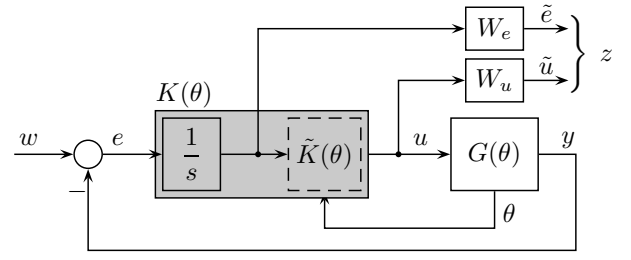


Fig. 2. Plant augmented with weighting functions.

In order to design the controller as previously described, it is necessary to define the augmented plant (10). That is, the interconnection between the plant and the controller where the performance signal z and the disturbance w are defined in accordance to the performance specifications. In the case of the PEMFC problem, the design can be posed as a typical mixed sensitivity problem. The main objective is to maintain the oxygen stoichiometry λ_{O_2} close to the reference value $\lambda_{O_2,ref}$, i.e., $e = \lambda_{O_2,ref} - \lambda_{O_2}$ and $w = \lambda_{O_2,ref}$; and in addition to keep limited the control action (compressor voltage) u . The controller output is saturated to ensure V_{cp} never exceeds the maximum and minimum levels. Therefore, the performance signal is given by $z = [\tilde{e} \ \tilde{u}]^T$, where tilde denotes the weighted version of these signals.

The augmented plant is shown in Figure 2, where $\tilde{K}(\theta)$ is the controller (11) produced by the synthesis procedure previously described. Integral action is included to ensure zero steady-state error. Thus, the weighting function W_e , which can be a simple constant, penalizes the error in low frequencies to guarantee the system operates at the desired set-point. On the other hand, the weight

$$W_u(s) = k_u \frac{10s/\omega_u + 1}{0.1s/\omega_u + 1}$$

penalizes the high frequency components of the control action. This weighting function also allows to consider the model (additive) uncertainty associated with the differences caused by the interpolation assumption and the theoretical model. The complete controller is thus given by $K(\theta) = (1/s) \cdot \tilde{K}(\theta)$, where \cdot stands for the series interconnection of two systems.

B. Discrete implementation

Finally, the continuous time controller (11) must be translated into a discrete time system for the implementation. This is not a trivial task in LPV systems because discretization changes the state space realizations and thus the parameter dependence of the LPV controller. To preserve the affine dependence, the system is discretized with Euler's forward method and the following approximation

$$e^{T_s A_c(\theta(kT_s))} \simeq I + T_s A_c(\theta(kT_s)),$$

where T_s is the sampling time [17]. With this approximation, the controller is expressed as

$$\begin{bmatrix} \dot{x}_c(k) \\ u(k) \end{bmatrix} = \sum_{i=1}^{m_1} \sum_{j=1}^{m_2} \alpha_{ij}(k) \begin{bmatrix} A_{d,ij} & T_s \bar{B}_{c,ij} \\ C_{c,ji} & D_{c,ij} \end{bmatrix} \begin{bmatrix} x_c(k) \\ e(k) \end{bmatrix} \quad (13)$$

in discrete time, where $A_{d,ij} = I + T_s \bar{A}_{c,ij}$.

IV. EXPERIMENTAL RESULTS

Considering the LPV description of the system introduced in Section III-A, the gain scheduled controller previously described was designed in a grid of 16 operating points given by

$$\mathcal{G} = \mathbf{V}_{cp,0} \times \mathbf{I}_{st,0},$$

with $\mathbf{V}_{cp,0} \in \{3, 6, 9, 12\}$ V and $\mathbf{I}_{st,0} \in \{2, 4, 6, 8\}$ A.

These values were selected after a sensitivity analysis of the system and in a way to get suitable points within the operating range of the fuel cell based system. This sensitivity analysis revealed that 16 points is a reasonable selection that accurately represents the system dynamical behavior, while keeping the parametrization and controller design within a relatively low level of complexity. The weighting functions in the synthesis were selected as

$$W_e(s) = 0.5, \quad W_u(s) = 0.005 \frac{s/0.3 + 1}{s/30 + 1}.$$

The latter function penalizes the control action in high frequencies and also provides robustness against differences between the model and the actual system. The controller was designed with an LMI pole placement region defined as:

$$\mathcal{E} = \left\{ s \in \mathbb{C} \mid -\frac{1}{10T_s} \leq \text{Re}(s) < 0 \cap |\text{Im}(s)| < \frac{1}{10T_s} \right\},$$

where T_s is the sampling time set at 10 ms. The order of the plant was reduced to 3, thus the controller order is 6. The optimization problem for obtaining the LPV controller was solved using Sedumi [18] and Yalmip [19].

The complete control strategy was implemented in the data acquisition and control system. It is composed of two computers (each with four cores i5 processor at 2.6 GHz clock frequency): the host and the real-time operating system (RTOS). The host provides the software development environment and the graphical user interface. It is responsible for the start up, shut down, configuration changes and control settings during operation. The RTOS implements the control algorithms and the data acquisition via a field-programmable gate array (FPGA), in order to have high speed data processing. Control, security and monitoring tasks are conducted by a CompactRIO (reconfigurable Input/Output) system from National Instruments. The LPV controller were developed in Matlab® and then cross-compiled into a LabView® environment. In order to record the analog sensor signals, a 32-channel 16-bit analog input module from National Instruments is used (NI-9205). A 8-channel, digital input/output (I/O) module generates the necessary transistor-transistor logic (TTL) signals for different security and diagnostic tools.

In order to evaluate the performance of the proposed LPV controller, two realistic and representative scenarios have been considered covering different working conditions and external disturbances.

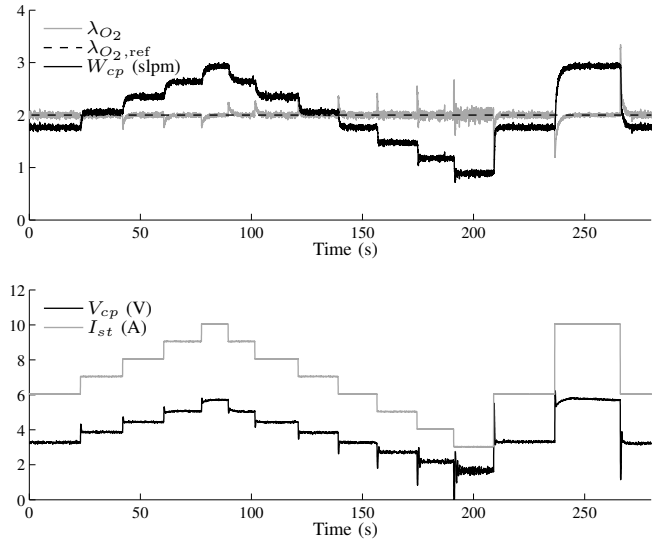


Fig. 3. Main variables related to test performed for Scenario 1.

A. Scenario 1

In an actual application, once the desired optimal value of $\lambda_{O_2,ref}$ is reached, it is interesting to evaluate the regulation behavior of the control system when current changes take place. To reproduce this typical working case, $\lambda_{O_2,ref}$ was set constant at 2, then different values of I_{st} were required from the PEMFC system. From this scenario, Figure 3 shows the behavior of the related variables. Here, several values of I_{st} are necessary in order to keep $\lambda_{O_2,ref}$ constant. Note the suitable regulation even for abrupt changes in I_{st} and for values of this current that were not taken into account neither in the model linearization nor in the controller design stage ($I_{st} = 10$ A from 240 to 265 s, approximately). This shows the robustness of the proposed control strategy. The noisy behavior of $\lambda_{O_2}(t)$ around 200 s (i.e., for $I_{st} = 3$ A) is due to the small value of the compressor flow, which is given in turn, by the voltage V_{cp} (control signal). Again, no peaks of λ_{O_2} below one were present despite the changes in I_{st} .

B. Scenario 2

Having verified the control operation in the nominal operation range, the system was then tested under the influence of external perturbations. This case may occur in practice when the cathode return manifold is throttled or an electronic valve is acting to keep constant the pressure between cathode and anode. In this particular test, I_{st} was kept constant at 6 A and an increment in the cathode's pressure $P_{cp}(t)$ was forced using a mechanical back pressure regulator (from 1.1 bar to 1.3 bar). This effect can be appreciated in Figure 4, where it is shown that from 20 to 110 s, while the valve is increasingly throttled, the reference tracking is successfully preserved. Next, when the valve is suddenly bypassed ($t = 110$ s), the system output departs from the reference but the LPV controller provides a quick recovery.

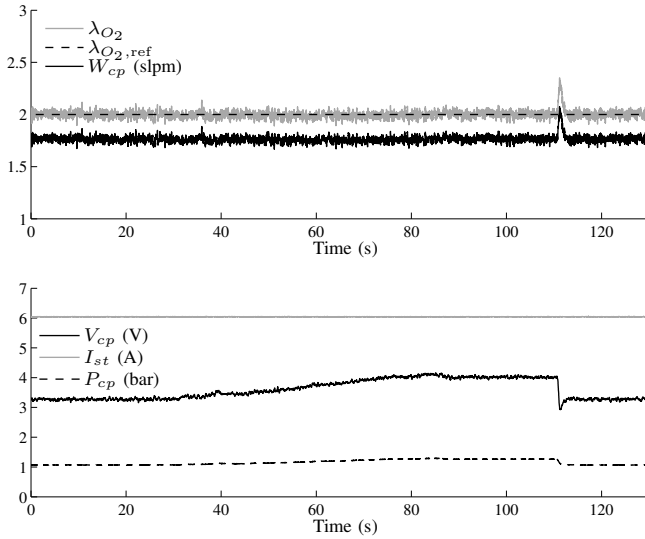


Fig. 4. Main variables related to test performed for Scenario 2.

V. CONCLUSIONS

An LPV gain scheduled control strategy has been proposed to regulate the oxygen stoichiometry of a PEMFC. A precise control of this variable is needed to ensure an efficient conversion and avoid irreversible damages in the polymeric membrane. Special attention has been paid to the implementation aspects. In addition, pole placement constraints have been considered in the LPV controller to guarantee a proper implementation in industrial computers. The complete control strategy has been implemented in an experimental platform and evaluated in a couple of representative scenarios. In all cases, the proposed control has exhibited promising results, maintaining the regulation of the oxygen stoichiometry despite the effect of the fluctuations in the load current. Future research efforts will be focused on the implementation of an anti-windup compensation for the LPV control scheme in order to mitigate the negative effects of the saturation of the control action.

ACKNOWLEDGEMENTS

All the experimental tests were performed at the PEM Fuel Cells Laboratory of the Institut de Robòtica i Informàtica Industrial (CSIC-UPC, Barcelona, Spain). The research of F.D. Bianchi was supported by the EIT and KIC-InnoEnergy under the Project SMART POWER (31.2011_IP27_Smart Power). The research of C. Kunusch has been supported by the Seventh Framework Programme of the European Community through the Marie Curie actions (GA: PCIG09-GA-2011-293876), the CICYT project DPI2011-25649 (MINECO-Spain) and the CSIC JAE-DOC Research Programme. The research of C. Ocampo-Martinez has been supported by the project MACPERCON (Ref. 201250E027) of the Spanish National Research Council (CSIC). The research of R.S. Sánchez Peña has been supported by CONICET and grant PICT2008-290 from the PRH Program

of the Ministry of Science, Technology and Innovation of Argentina.

REFERENCES

- [1] "Department of Energy. Hydrogen, Fuel Cells And Infrastructure Technologies Program: Multi-Year Research, Development And Demonstration Plan: planned program activities for 2005-2015. DOE Website. Section 3.4 Fuel Cells." Tech. Rep., 2005.
- [2] J. Pukrushpan, A. Stefanopoulou, and H. Peng, *Control of Fuel Cell Power Systems*. Springer, 2004.
- [3] J. Larminie and A. Dicks, *Fuel Cell Systems Explained*, 2nd ed. John Wiley & Sons Inc, 2003.
- [4] J. Gruber, C. Bordons, and A. Oliva, "Nonlinear MPC for the airflow in a PEM fuel cell using a volterra series model," *Control Engineering Practice*, vol. 20, no. 2, pp. 205–217, 2012.
- [5] A. Arce, A. del Real, C. Bordons, and D. Ramirez, "Real-time implementation of a constrained mpc for efficient airflow control in a pem fuel cell," *IEEE Trans. on Industrial Electronics*, vol. 57, no. 6, pp. 1892–1905, 2010.
- [6] A. Accetta, M. Cirrincione, G. Marsala, M. Pucci, and G. Vitale, "Pem fuel cell system model predictive control and real-time operation on a power emulator," in *IEEE Energy Conversion Congress and Exposition (ECCE)*, 2010, pp. 1610–1616.
- [7] B. M. Sanandaji, T. L. Vincent, A. Colclasure, and R. J. Kee, "Control-oriented modeling of a solid-oxide fuel cell stack using an LPV model structure," in *Proc. of the Dynamic Systems and Control Conference*, 2009, pp. 793–800.
- [8] D. Hernandez-Torres, "Commande robuste de générateurs électrochimiques hybrides," Ph.D. dissertation, Université de Grenoble, Grenoble, France, 2011.
- [9] D. Hernandez-Torres, O. Sename, and D. Riu, "An LPV control approach for a fuel cell power generator air supply system," in *Proc. of the American Control Conference*, 2012.
- [10] S. D. Lira, V. Puig, J. Quevedo, and A. Husar, "LPV observer design for pem fuel cell system: Application to fault detection," *Journal of Power Sources*, vol. 196, no. 9, pp. 4298–4305, 2011.
- [11] C. Kunusch, P. Puleston, M. Mayosky, and A. Husar, "Control oriented modelling and experimental validation of a PEMFC generation system," *IEEE Trans. on Energy Conversion*, vol. 6, no. 3, pp. 851–861, 2011.
- [12] C. Kunusch, P. Puleston, and M. Mayosky, *Sliding-Mode Control of PEM Fuel Cells*. Springer UK, 2012.
- [13] M. Chilali and P. Gahinet, " H_∞ design with pole placement constraints: an LMI approach," *IEEE Trans. on Automatic Control*, vol. 41, no. 3, pp. 358–367, 1996.
- [14] P. Apkarian and R. Adams, "Advanced gain-scheduling techniques for uncertain systems," *IEEE Trans. on Control Systems Technology*, vol. 6, no. 1, pp. 21–32, 1998.
- [15] S. Lim and J. P. How, "Modeling and H_∞ control for switched linear parameter-varying missile autopilot," *IEEE Trans. on Control Systems Technology*, vol. 11, no. 6, pp. 830–838, 2003.
- [16] F. Wu, X. H. Yang, A. Packard, and G. S. Becker, "Induced L_2 -norm control for LPV systems with bounded parameter variation rates," *Int. Journal of Robust and Nonlinear Control*, vol. 6, pp. 983–998, 1996.
- [17] R. Toth, P. S. Heuberger, and P. M. Van Den Hof, "Discretisation of linear parameter-varying state-space representations," *IET Control Theory & Applications*, vol. 4, no. 10, pp. 2082–2096, 2010.
- [18] J. Sturm, "Using SeDuMi 1.02, a Matlab toolbox for optimization over symmetric cones," *Optim. Method Softw.*, vol. 11-12, pp. 625–653, 1999.
- [19] J. Löfberg, "Yalmip : A toolbox for modeling and optimization in MATLAB," in *Proc. of the CACSD Conference*, Taipei, Taiwan, 2004.